

AD-A071 315

AIR FORCE WEAPONS LAB KIRTLAND AFB NM
MODELING STUDIES OF THE MIXING AND CHEMISTRY OF THE NF RADICALS--ETC(U)
JUN 79 R A ARMSTRONG, N L RAPAGNANI
AFWL-TR-78-263

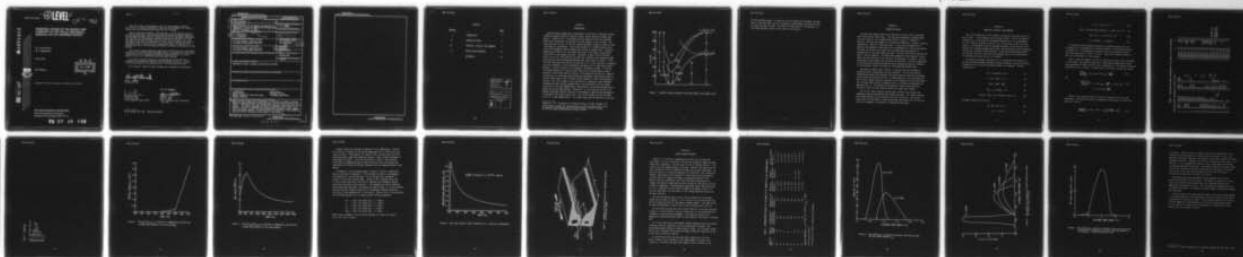
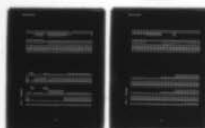
F/G 20/5

UNCLASSIFIED

NL

1 OF 1

AD
A071315



END
DATE
FILMED

8-79

DDC

AFWL-TR-78-263

② LEVEL II

AFWL-TR-78-263

DDC

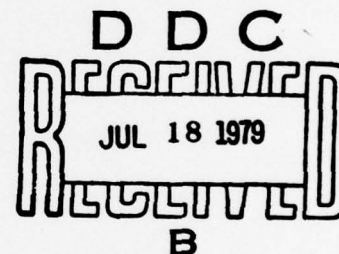
DA071315

MODELING STUDIES OF THE MIXING AND
CHEMISTRY OF THE $NF(a'\Delta)$ AND $NF(b'\Sigma)$
RADICALS ON THE TRISTREAM NOZZLE

R. A. Armstrong
N. L. Rapagnani

June 1979

Final Report



DDC FILE COPY

Approved for public release; distribution unlimited.

AIR FORCE WEAPONS LABORATORY
Air Force Systems Command
Kirtland Air Force Base, NM 87117

79 07 16 140

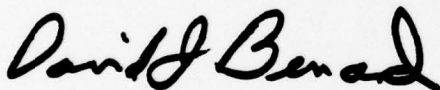
This final report was prepared by the Air Force Weapons Laboratory, Kirtland Air Force Base, New Mexico, under Job Order 33260392. Mr. David J. Benard (ALC) was the Laboratory Project Officer-in-Charge.

When US Government drawings, specifications, or other data are used for any purpose other than a definitely related Government procurement operation, the Government thereby incurs no responsibility nor any obligation whatsoever, and the fact that the Government may have formulated, furnished, or in any way supplied the said drawings, specifications, or other data is not to be regarded by implication or otherwise as in any manner licensing the holder or any other person or corporation or conveying any rights or permission to manufacture, use or sell any patented invention that may in any way be related thereto.

This report has been authored by employees of the United States Government. Accordingly, the United States Government retains a nonexclusive, royalty-free license to publish or reproduce the material contained herein, or allow others to do so, for the United States Government purposes.

This report has been reviewed by the Information Office (OI) and is releasable to the National Technical Information Service (NTIS). At NTIS, it will be available to the general public, including foreign nations.

This technical report has been reviewed and is approved for publication.

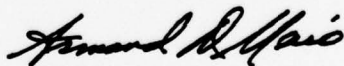


DAVID J. BENARD
Project Officer



DAVID S. OLSON
Lt Colonel, USAF
Chief, Chemical Laser Branch

FOR THE COMMANDER



ARMAND D. MAIO
Colonel, USAF
Chief, Advanced Laser Technology
Division

DO NOT RETURN THIS COPY. RETAIN OR DESTROY.

UNCLASSIFIED

SECURITY CLASSIFICATION OF THIS PAGE (When Data Entered)

| REPORT DOCUMENTATION PAGE | | READ INSTRUCTIONS BEFORE COMPLETING FORM |
|--|--|---|
| 1. REPORT NUMBER AFWL-TR-78-263 | 2. GOVT ACCESSION NO. | 3. RECIPIENT'S CATALOG NUMBER |
| 4. TITLE (and Subtitle) MODELING STUDIES OF THE MIXING AND CHEMISTRY OF THE $NF(a_1^4)$ AND $NF(b_1^3\Sigma)$ RADICALS ON THE TRISTREAM NOZZLE. <i>Delta</i> <i>sigma</i> | 5. TYPE OF REPORT & PERIOD COVERED Final Report | |
| 7. AUTHOR(s) R. A. Armstrong N. L. Rapagnani | 8. CONTRACT OR GRANT NUMBER(s) 15 26 p | |
| 9. PERFORMING ORGANIZATION NAME AND ADDRESS Air Force Weapons Laboratory (ALC) Kirtland Air Force Base, NM 87117 | 10. PROGRAM ELEMENT, PROJECT, TASK AREA & WORK UNIT NUMBERS 62601F/33260392 16 17 03 | |
| 11. CONTROLLING OFFICE NAME AND ADDRESS Air Force Weapons Laboratory (ALC) Kirtland Air Force Base, NM 87117 | 12. REPORT DATE June 1979 | |
| 14. MONITORING AGENCY NAME & ADDRESS (if different from Controlling Office) | 13. NUMBER OF PAGES 24 | |
| | 15. SECURITY CLASS. (of this report) UNCLASSIFIED | |
| | 15a. DECLASSIFICATION/DOWNGRADING SCHEDULE | |
| 16. DISTRIBUTION STATEMENT (of this Report) Approved for public release; distribution unlimited. | | |
| 17. DISTRIBUTION STATEMENT (of the abstract entered in Block 20, if different from Report) | | |
| 18. SUPPLEMENTARY NOTES | | |
| 19. KEY WORDS (Continue on reverse side if necessary and identify by block number) 2-Dimensional Laser Nozzle Laminar Mixing Nitrogen Fluoride Chemical Electronic Transition Laser Tristeam Laser Nozzle Computer Modeling | | |
| 20. ABSTRACT (Continue on reverse side if necessary and identify by block number) Among the many systems being investigated in the effort to develop a thermo-chemically pumped electronic transition laser, the NF radical has shown high promise. This report describes the modeling completed to evaluate an NF mixing concept. Calculations were made with varying expansion ratios, both in the nozzle and cavity, to determine the optimum throat pressures, throat temperatures and element lengths. The mixing concept as described is very promising and could lase if the optical path length is long enough. | | |

DD FORM 1 JAN 73 1473 EDITION OF 1 NOV 65 IS OBSOLETE

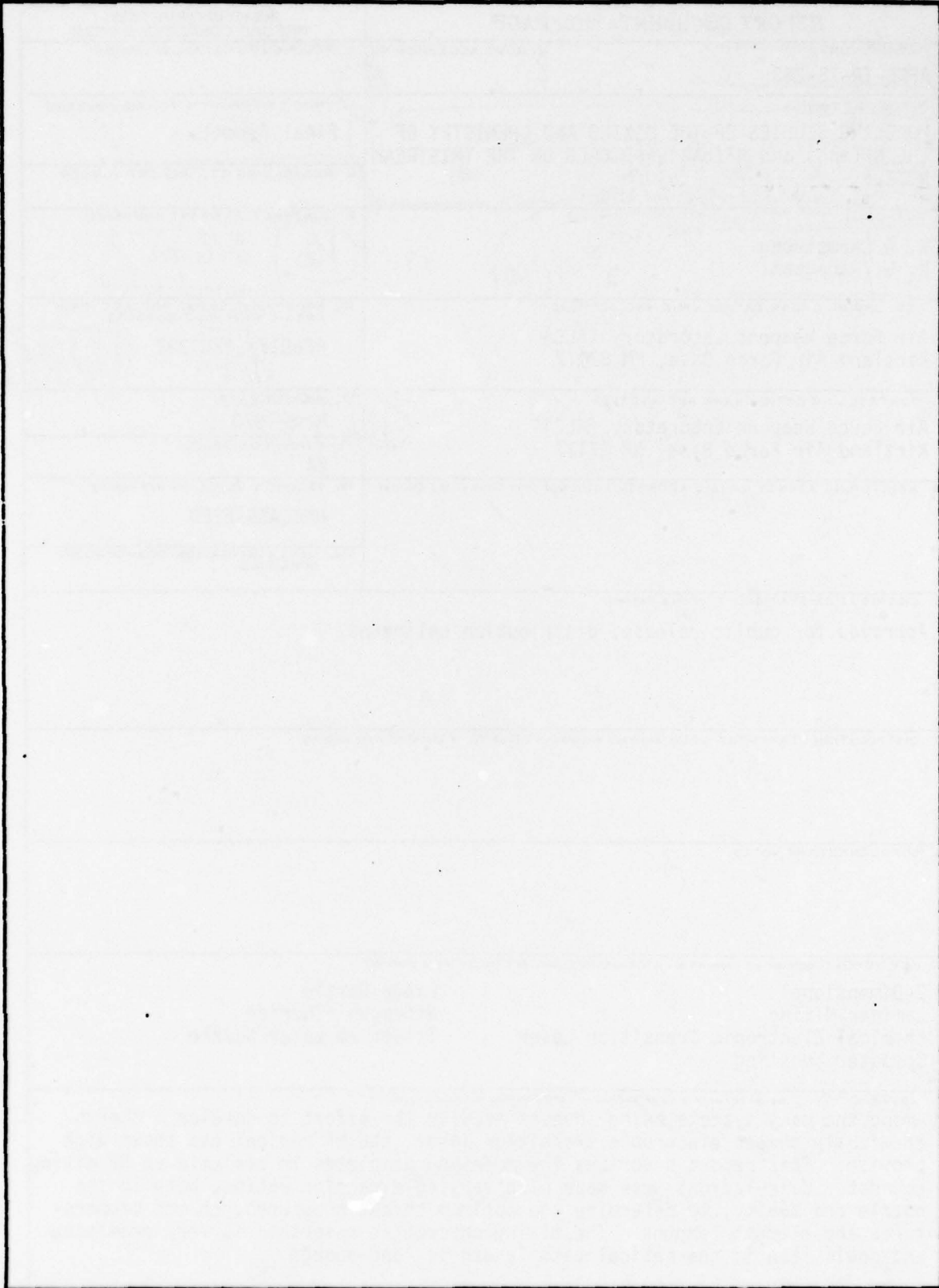
UNCLASSIFIED

SECURITY CLASSIFICATION OF THIS PAGE (When Data Entered)

013 150

UNCLASSIFIED

SECURITY CLASSIFICATION OF THIS PAGE(When Data Entered)



UNCLASSIFIED

SECURITY CLASSIFICATION OF THIS PAGE(When Data Entered)

CONTENTS

| <u>Section</u> | | <u>Page</u> |
|----------------|-----------------------------------|-------------|
| I | INTRODUCTION | 3 |
| II | THEORETICAL MODEL | 6 |
| III | CHEMISTRY, KINETICS, AND HARDWARE | 7 |
| IV | RESULTS AND DISCUSSION | 18 |
| | REFERENCES | 24 |

| | |
|---------------------|--|
| Accession For | |
| NTIS GRA&I | <input checked="checked" type="checkbox"/> |
| DDC TAB | <input type="checkbox"/> |
| Unannounced | <input type="checkbox"/> |
| Justification _____ | |
| By _____ | |
| Distribution/ _____ | |
| Availability Codes | |
| Dist. | Avail and/or special |
| A | |

SECTION I

INTRODUCTION

Among the many systems being investigated in the effort to develop a thermochemically pumped electronic transition laser, the NF radical has shown high promise. Herbelin (ref. 1) has shown that the reaction of NF_2 with hydrogen atoms yields essentially 100 percent of the NF product in the $a^1\Delta$ state. The reason he gives for this is that the reaction proceeds through a relatively long lived $\text{HNF}_2(^1\text{A})$ intermediate. Since the HF product is a singlet state by spin correlation arguments, the NF product must also be a singlet state. Since the ground state of NF is $X^3\Sigma$, the product must form in the lowest lying singlet state which is the excited $a^1\Delta$ state. Therefore, a total initial inversion exists on the $a^1\Delta \rightarrow X^3\Sigma$ transition at 874.2 nm. Herbelin* has presented an RKR calculation on the NF system and generated the curves shown in figure 1. Note that the transitions are vertical so that the $(v', v'' = 0, 0)$ transition is expected to be the strongest, a fact that Herbelin and Kwok (ref. 2) have proven experimentally. Also of interest in this system is the $\text{NF}(b^1\Delta)$ system. If one can efficiently produce this state (a point that we will discuss later), a more attractive laser could result on the $b^1\Sigma \rightarrow X^3\Sigma$ transition at 528.8 nm. Herbelin and Kwok (ref. 2) have done some preliminary experiments which indicate that if the $X^3\Sigma$ ground state of NF is formed in their system it is well below detection limited. Thus, this system is very attractive as a potential laser candidate. Although much work has been accomplished in the evaluation of the NF system, lasing has not yet been demonstrated. Additionally, the optimum hardware/nozzle design has not yet been decided. Discussions on this point at the Air Force Weapons Laboratory (AFWL)** resulted in the concept of applying the Rocketdyne's tristream HF laser nozzle design (ref. 3) to the NF system, to test the feasibility of a laser demonstration. This report describes the modeling to evaluate

*Herbelin, J. M., Presentation of Technical Review to AFWL, November 1977.

**The original concept for the application of the tristream nozzle to the NF chemical laser program arose from discussions principally between Lt Col Carl Forbrich and Capt Paul Flynn, of AFWL.

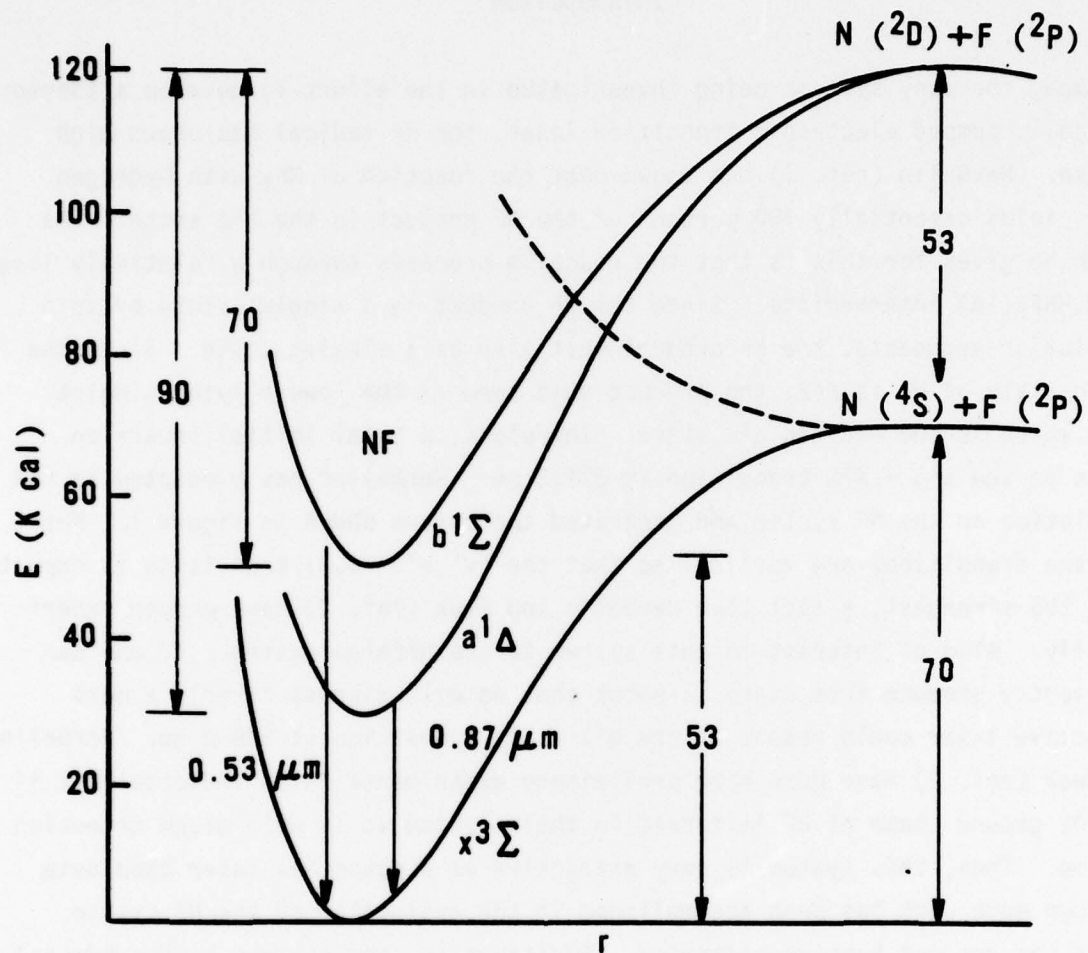


Figure 1. Potential energy diagram of the three lowest lying states of NF.

the NF/tristream concept. In addition, the tristream nozzle hardware has been given to TRW under AFWL contract to develop an experimental data base on which to anchor the modeling code. The results of that work will be reported in a later AFWL technical report at the close of the contract.

SECTION II

THEORETICAL MODEL

The main tool used to perform the theoretical analysis was the Advanced Laser Flow Analysis (ALFA) code. This code was developed by Lockheed under Air Force contract, and a complete description is given in reference 4. Basically, ALFA has the capability to handle two-dimensional, viscous, reactive, compressible, laminar or turbulent flows. It also has the capability of handling flow expansion either parallel or perpendicular to the mixing regions. This gave us the ability to model the tristream where the expansion is perpendicular to the reacting/mixing zones. The only modification required was that of the gain equation. The ALFA code assumed the lasing species is polyatomic and the transition to be vibronic, not electronic, in nature. Thus to investigate the NF system, the code had to be modified. This was accomplished by inserting the derived gain equation and by changing the heat of formation of the electronic states to account for the energy gap between them.

The code can handle either laminar or turbulent (by the two-equation turbulent kinetic energy model) mixing flowfields. All the calculations presented were done using turbulent mixing and some were done (not presented) using laminar (diffusional) mixing. At these pressures, one can assume that the flow will become turbulent; therefore, for Rocketdyne to effectively model the tristream (when used as a chemical laser), a turbulent mixing model was employed (ref. 3). The laminar mixing peak gain results were typically 25 percent lower than the turbulent cases with longer gain lengths.

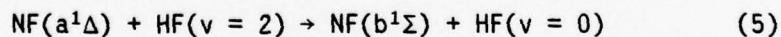
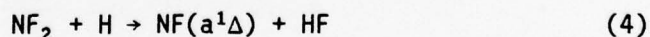
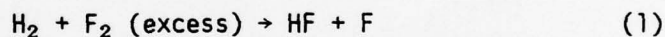
The initial lateral species profiles were uniform, with velocity and temperature defects assumed near the element divisions. The lateral pressure was assumed constant but calculated in the axial direction. This type of model had sufficient detail in the mixing zones which would give us realistic results as compared to a premixed or scheduled mixing model.

SECTION III

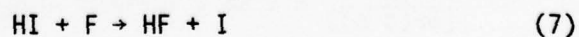
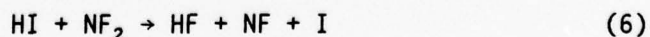
CHEMISTRY, KINETICS, AND HARDWARE

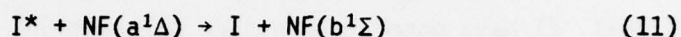
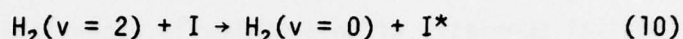
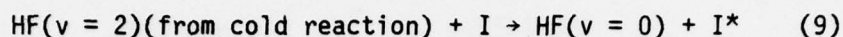
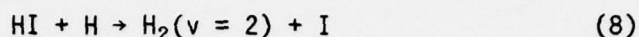
The initial chemistry of this system is essentially the same as that for the HF laser. If one produces fluorine atoms, either in an arc as Herbelin and Kwok (ref. 2) have done at Aerospace Corporation, or in a precombustor HF "hot" reaction as Betts and Miller (ref. 5) have done at TRW, and react them in a stoichiometric mix with hydrogen molecules, the ensuing HF "cold" reaction will produce hydrogen atoms, heat, and vibrationally hot HF molecules. The heat will thermally dissociate N_2F_4 , introduced through adjacent ports, to form NF_2 , which will react with the hydrogen atoms to form the $NF(a^1\Delta)$. Two secondary reactions are also of interest.

The results of Herbelin and Kwok (ref. 2) showed that the reaction of $HF(v+2)$ with $NF(a^1\Delta)$ pumps the $NF(b^1\Sigma)$ state with about 1 percent efficiency. Introduction of HI with the hydrogen increases this pumping. The main reactions are:



Secondary reactions with HI are





The groups at both Aerospace Corporation and TRW have shown that the introduction of HI dramatically increases the $\text{NF}(b^1\Sigma \rightarrow X^3\Sigma)$ emission because of reaction 11. The sequential reactions 8 and 10 are probably the most efficient producers of I^* (refs. 5 and 6). These basic reactions form the basis for investigation of this system.

Table 1 shows the complete listing of reactions and their rates considered in this study. The reaction rates were in some cases estimated and in most cases measured and came principally from a compilation of rate data by Aerospace Corporation (refs. 7 and 8). A steady state rate analysis yields the results

$$\frac{[\text{NF}_2]_{ss}}{[\text{N}_2\text{F}_4]_{ss}} = 8.2 \times 10^{-6} T^{3/2} \exp \frac{-15200}{RT} \quad (12)$$

and

$$\begin{aligned} \frac{[\text{NF}(a^1\Delta)]_{ss}}{[\text{NF}_2]_{ss}} &= 1 \times 10^{13} \exp \frac{-3000}{RT} + 3.78 \times 10^{11} \quad (13) \\ &+ 1.0 \times 10^{13} \exp \frac{-4000}{RT} \end{aligned}$$

Figures 2 and 3 show the results of plots of equations 12 and 13 with temperature. An additional effect of temperature can be seen in the derived gain cross section,

$$\frac{\gamma(\text{cm}^{-1})}{[\text{NF}(a^1\Delta)]} = 4.44 \times 10^{-18} T^{-1} \exp \left[\frac{0.4425}{T} - 0.5 \right] \quad (14)$$

TABLE 1. REACTIONS AND RATES CONSIDERED IN THE MODEL OF THE NF CHEMISTRY

| REACTIONS BEING CONSIDERED $[K=AT^N \exp(-B/RT)]$ | | A | N | B |
|---|--|--|-----------|------|
| 1 | HF(2) + NF(A) | HF(0) + NF(B) | 3.162E+11 | -50 |
| 2 | HF(3) + NF(A) | HF(1) + NF(B) | 2.506E+12 | -50 |
| 3 | H + NF(B) | HF(0) + N | 1.988E+13 | -50 |
| 4 | N + NF(B) | N ₂ + F | 3.981E+12 | -50 |
| 5 | NF(B) + NF(B) | N ₂ + F + F | 9.999E+11 | -50 |
| 6 | NF(B) + NF(A) | N ₂ + F + F | 9.999E+11 | -50 |
| 7 | NF(X) + NF(A) | N ₂ + F + F | 9.999E+11 | -50 |
| 8 | H + NF ₂ | HF(0) + NF(A) | 9.999E+12 | -50 |
| 9 | H + NF(A) | HF(0) + N | 9.999E+12 | -50 |
| 10 | H + NF(X) | HF(0) + N | 9.999E+12 | -50 |
| 11 | N + NF ₂ | N ₂ + F + F | 2.512E+12 | -50 |
| 12 | N + NF(X) | N ₂ + F | 4.017E+12 | -50 |
| 13 | N + NF(A) | N ₂ + F | 3.981E+12 | -50 |
| 14 | NF(X) + NF(X) | N ₂ + F + F | 9.999E+11 | -50 |
| 15 | NF(A) + NF(A) | N ₂ + F + F | 9.999E+11 | -50 |
| 16 | NF(A) + NF(X) | N ₂ + F + F | 9.999E+11 | -50 |
| 17 | NF(A) + NF ₂ | N ₂ F ₂ + F | 9.999E+11 | -50 |
| 18 | NF(X) + NF ₂ | N ₂ F ₂ + F | 9.999E+11 | -50 |
| 19 | N ₂ F ₂ + NF ₂ | NF ₃ + F | 9.999E+11 | -50 |
| 20 | NF ₃ + N ₂ | NF ₂ + F + M ₂ | 3.981E+16 | -50 |
| 21 | NF(A) + H ₂ (0) | NF(X) + H ₂ (0) | 3.999E+10 | 0.00 |
| 22 | N ₂ F ₄ + M ₁ | NF ₂ + NF ₂ + M ₁ | 1.506E+15 | -50 |
| 23 | NF ₂ + NF ₂ + M ₁ | N ₂ F ₄ + M ₁ | 2.402E+18 | 1.00 |
| 24 | NF ₂ + F + M ₂ | NF ₃ + M ₂ | 8.997E+19 | 1.00 |
| 25 | NF(a) + I* | NF(B) + I | 2.590E+14 | 0.00 |
| 26 | H + H ₂ | H ₂ (2) + I | 1.385E+12 | -50 |
| 27 | HF(2) + I | HF(0) + I* | 1.301E+12 | 0.00 |
| 28 | H ₂ (2) + I | H ₂ (0) + I* | 4.999E+12 | 0.00 |
| 29 | I + F ₂ | IF + F | 4.999E+14 | 0.00 |
| 30 | I* + F ₂ | IF + F | 4.999E+14 | 0.00 |

FORWARD ONLY

FORWARD ONLY

FORWARD ONLY

TABLE 1. CONTINUED

| | | | | | |
|----|-------------|--------------|-----------|-------|---------|
| 31 | HF(1) + I* | = HF(3) + I | 3.198E+12 | 0.00 | 0.0 |
| 32 | HF(2) + I* | = HF(4) + I | 8.312E+11 | 0.00 | 0.0 |
| 33 | I* + M13 | = I + M13 | 5.602E+19 | 0.00 | 0.0 |
| 34 | I + I + M13 | = 12 + M13 | 1.342E+16 | 0.00 | 0.0 |
| 35 | I* + I + M1 | = 12 + M1 | 1.451E+15 | 0.00 | 0.0 |
| 36 | F + HI | = HF(0) + I | 9.999E+12 | 0.00 | -1400.0 |
| 37 | F + HI | = HF(1) + I | 1.301E+13 | 0.00 | -1400.0 |
| 38 | F + HI | = HF(2) + I | 1.500E+13 | 0.00 | -1400.0 |
| 39 | F + HI | = HF(3) + I | 1.602E+13 | 0.00 | -1400.0 |
| 40 | F + HI | = HF(4) + I | 2.000E+13 | 0.00 | -1400.0 |
| 41 | H + H + M1 | = H2(0) + M1 | 6.204E+17 | .95 | 0.0 |
| 42 | H + H + M6 | = H2(0) + M6 | 9.396E+16 | .61 | 0.0 |
| 43 | F + F + M2 | = F2 + M2 | 4.716E+15 | 1.00 | 1250.0 |
| 44 | F + H2(0) | = HF(1) + H | 2.722E+13 | 0.00 | -1600.0 |
| 45 | F + H2(1) | = HF(1) + H | 2.722E+13 | 0.00 | -1600.0 |
| 46 | F + H2(2) | = HF(1) + H | 2.722E+13 | 0.00 | -1600.0 |
| 47 | F + H2(0) | = HF(2) + H | 8.794E+13 | 0.00 | -1600.0 |
| 48 | F + H2(1) | = HF(2) + H | 8.794E+13 | 0.00 | -1600.0 |
| 49 | F + H2(2) | = HF(2) + H | 8.794E+13 | 0.00 | -1600.0 |
| 50 | F + H2(0) | = HF(3) + H | 4.481E+13 | 0.00 | -1600.0 |
| 51 | F + H2(1) | = HF(3) + H | 4.481E+13 | 0.00 | -1600.0 |
| 52 | F + H2(2) | = HF(3) + H | 4.481E+13 | 0.00 | -1600.0 |
| 53 | HF(4) + H | = H2(0) + F | 3.704E+12 | 0.00 | -460.0 |
| 54 | HF(4) + H | = H2(1) + F | 3.704E+12 | 0.00 | -460.0 |
| 55 | HF(1) + MS | = HF(0) + MS | 2.945E+14 | 1.00 | 0.0 |
| 56 | HF(1) + MS | = HF(0) + MS | 3.499E+04 | -2.26 | 0.0 |
| 57 | HF(2) + MS | = HF(1) + MS | 5.891E+14 | 1.00 | 0.0 |
| 58 | HF(2) + MS | = HF(1) + MS | 6.987E+04 | 2.26 | 0.0 |
| 59 | HF(2) + MS | = HF(0) + MS | 7.469E+14 | 1.00 | 0.0 |
| 60 | HF(3) + M5 | = HF(2) + M5 | 8.854E+14 | 1.00 | 0.0 |
| 61 | HF(3) + M5 | = HF(2) + M5 | 1.048E+05 | -2.26 | 0.0 |
| 62 | HF(3) + M5 | = HF(1) + M5 | 1.494E+15 | 1.00 | 0.0 |
| 63 | HF(3) + M5 | = HF(0) + M5 | 9.999E+14 | 1.00 | 0.0 |
| 64 | HF(4) + M5 | = HF(3) + M5 | 1.181E+15 | 1.00 | 0.0 |
| 65 | HF(4) + M5 | = HF(3) + M5 | 1.343E+05 | -2.26 | 0.0 |
| 66 | HF(4) + M5 | = HF(2) + M5 | 2.241E+15 | 1.00 | 0.0 |
| 67 | HF(4) + M5 | = HF(1) + M5 | 1.500E+15 | 1.00 | 0.0 |
| 68 | HF(1) + H | = HF(0) + H | 4.517E+11 | 0.00 | -700.0 |

TABLE 1. CONTINUED

| | | | | | |
|-----|---------------|-----------------|-----------|-------|---------|
| 69 | HF(2) + H | = HF(1) + H | 8.432E+12 | 0.00 | -700.0 |
| 70 | HF(2) + H | = HF(0) + H | 4.216E+12 | 0.00 | -700.0 |
| 71 | HF(3) + H | = HF(2) + H | 1.566E+14 | 0.00 | -700.0 |
| 72 | HF(3) + H | = HF(1) + H | 7.830E+12 | 0.00 | -700.0 |
| 73 | HF(3) + H | = HF(0) + H | 5.180E+12 | 0.00 | -700.0 |
| 74 | HF(4) + H | = HF(3) + H | 1.807E+14 | 0.00 | -700.0 |
| 75 | HF(4) + H | = HF(2) + H | 1.385E+14 | 0.00 | -700.0 |
| 76 | HF(4) + H | = HF(1) + H | 9.035E+13 | 0.00 | -700.0 |
| 77 | HF(1) + F | = HF(0) + F | 4.819E+15 | .75 | -3600.0 |
| 78 | HF(2) + F | = HF(1) + F | 1.927E+16 | .75 | -3600.0 |
| 79 | HF(2) + F | = HF(0) + F | 9.637E+15 | .75 | -3600.0 |
| 80 | HF(3) + F | = HF(2) + F | 4.337E+16 | .75 | -3600.0 |
| 81 | HF(3) + F | = HF(1) + F | 2.168E+16 | .75 | -3600.0 |
| 82 | HF(3) + F | = HF(0) + F | 1.446E+16 | .75 | -3600.0 |
| 83 | HF(4) + F | = HF(3) + F | 7.830E+16 | .75 | -3600.0 |
| 84 | HF(4) + F | = HF(2) + F | 3.855E+16 | .75 | -3600.0 |
| 85 | HF(4) + F | = HF(1) + F | 2.590E+16 | .75 | -3600.0 |
| 86 | HF(1) + M8 | = HF(0) + M8 | 5.999E+07 | -1.00 | 0.0 |
| 87 | HF(2) + M8 | = HF(1) + M8 | 1.199E+08 | -1.00 | 0.0 |
| 88 | HF(3) + M8 | = HF(2) + M8 | 1.801E+08 | -1.00 | 0.0 |
| 89 | HF(4) + M8 | = HF(3) + M8 | 2.397E+08 | -1.00 | 0.0 |
| 90 | HF(1) + M7 | = H2(0) + M7 | 2.500E-04 | -4.30 | 0.0 |
| 91 | H2(2) + M7 | = H2(1) + M7 | 4.999E-04 | -4.30 | 0.0 |
| 92 | H2(1) + M9 | = H2(0) + M9 | 2.000E+13 | 0.00 | -2720.0 |
| 93 | H2(2) + M9 | = H2(1) + M9 | 2.000E+13 | 0.00 | -2720.0 |
| 94 | HF(1) + HF(1) | = HF(0) + HF(2) | 3.000E+15 | 1.00 | 0.0 |
| 95 | HF(2) + HF(2) | = HF(1) + HF(3) | 3.000E+15 | 1.00 | 0.0 |
| 96 | HF(3) + HF(3) | = HF(2) + HF(4) | 3.000E+15 | 1.00 | 0.0 |
| 97 | HF(1) + HF(2) | = HF(0) + HF(3) | 3.000E+15 | 1.00 | 0.0 |
| 98 | HF(2) + HF(3) | = HF(1) + HF(4) | 3.000E+15 | 1.00 | 0.0 |
| 99 | HF(1) + HF(3) | = HF(0) + HF(4) | 3.000E+15 | 1.00 | 0.0 |
| 100 | HF(0) + HF(1) | = HF(1) + H2(0) | 9.035E+11 | 0.00 | 0.0 |
| 101 | HF(0) + H2(2) | = HF(1) + H2(1) | 9.035E+11 | 0.00 | 0.0 |
| 102 | HF(1) + H2(1) | = HF(2) + H2(0) | 2.891E+12 | 0.00 | 0.0 |
| 103 | HF(1) + H2(2) | = HF(2) + H2(1) | 2.891E+12 | 0.00 | 0.0 |
| 104 | HF(2) + H2(1) | = HF(3) + H2(0) | 9.035E+12 | 0.00 | 0.0 |
| 105 | HF(2) + H2(2) | = HF(3) + H2(1) | 9.035E+12 | 0.00 | 0.0 |
| 106 | HF(3) + H2(1) | = HF(4) + H2(0) | 1.988E+12 | 0.00 | 0.0 |
| 107 | HF(3) + H2(2) | = HF(4) + H2(1) | 1.988E+13 | 0.00 | 0.0 |

TABLE 1. CONCLUDED

M1 = All other species
M22 = He
M6 = 20H, H₂
M2 = all with 2, 7xF₂
M5 = All HF Species
M8 = H₂, He
M7 = H₂, H
M9 = H
M13 = I₂

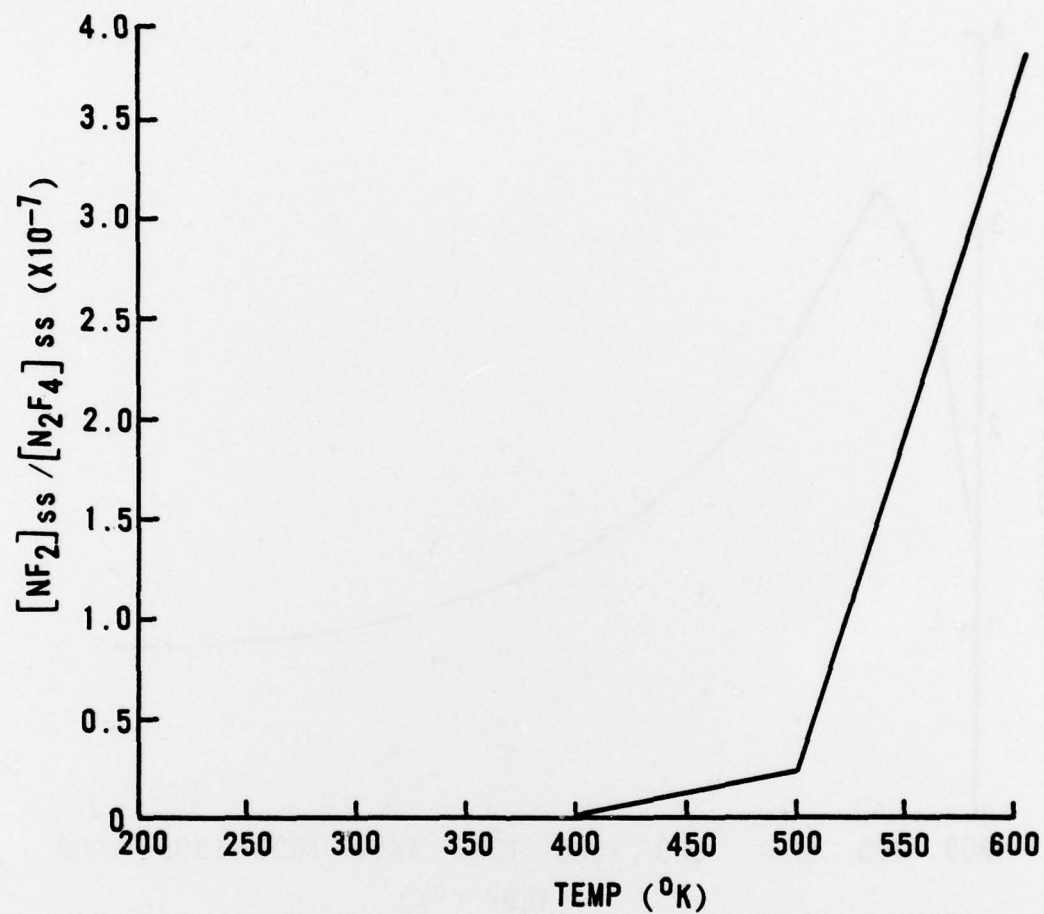


Figure 2. $[NF_2]_{ss}/[N_2F_4]_{ss}$ as a function of temperature, derived from a steady state analysis of the rate package.

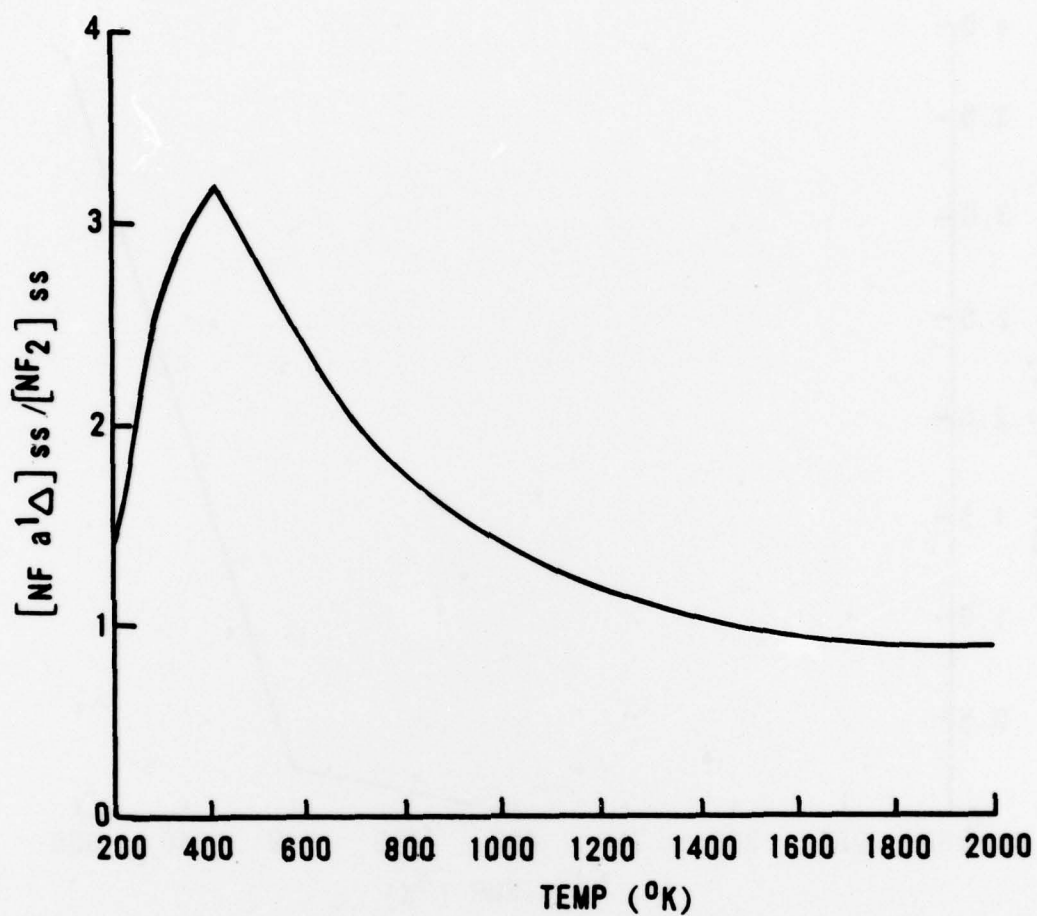


Figure 3. $[NF(a^1\Delta)]_{ss}/[NF_2]_{ss}$ as a function of temperature, derived from a steady state analysis of the rate package.

Figure 4 shows the variation of equation 14 with temperature. The gain cross section increases with decreasing temperature due to diminishing rotational dilution. Unfortunately, as figure 2 shows, the N_2F_4 does not dissociate below 600 K under the conditions studied. Figure 3 shows a maximum in the $[NF(a^1\Delta)]$ at 500 K. Since the dissociation of N_2F_4 is the necessary first step, the temperature must be kept relatively high, which means that conditions are off peak for $NF(a^1\Delta)$ production and the commensurate gain cross section.

A schematic of the tristream concept is shown in figure 5; dimensional details are given in reference 3. The tristream is mated to a precombustor for production of the fluorine atom. The H_2 and N_2F_4 are introduced in parallel flow to the fluorine atoms. The N_2F_4 flow is between the H_2 and F flows so that diffusion of the initial reactants and subsequent heating would more efficiently dissociate N_2F_4 . The subsequent mixing and chemistry have already been described. We defined an element length, L_e , as the distance from the fluorine injector centerline to the hydrogen injector centerline, since this is the repeating unit in the nozzle. Typical initial flow conditions for the throat pressure of a 0.5 atm case were (from precombustor)

| | | | |
|----------|---|---|--------------|
| DF | - | 7.96×10^{-4} moles sec^{-1} , | $T = 1450$ K |
| F | - | 7.96×10^{-4} moles sec^{-1} , | $T = 1450$ K |
| He | - | 2.39×10^{-3} moles sec^{-1} , | $T = 1450$ K |
| H_2 | - | 1.25×10^{-3} moles sec^{-1} , | $T = 300$ K |
| N_2F_4 | - | 1.89×10^{-3} moles sec^{-1} , | $T = 300$ K |

When HI was introduced, it was with the hydrogen at a molar flow rate of $4.18 \times 10^{-4} \text{ sec}^{-1}$ at 300 K.

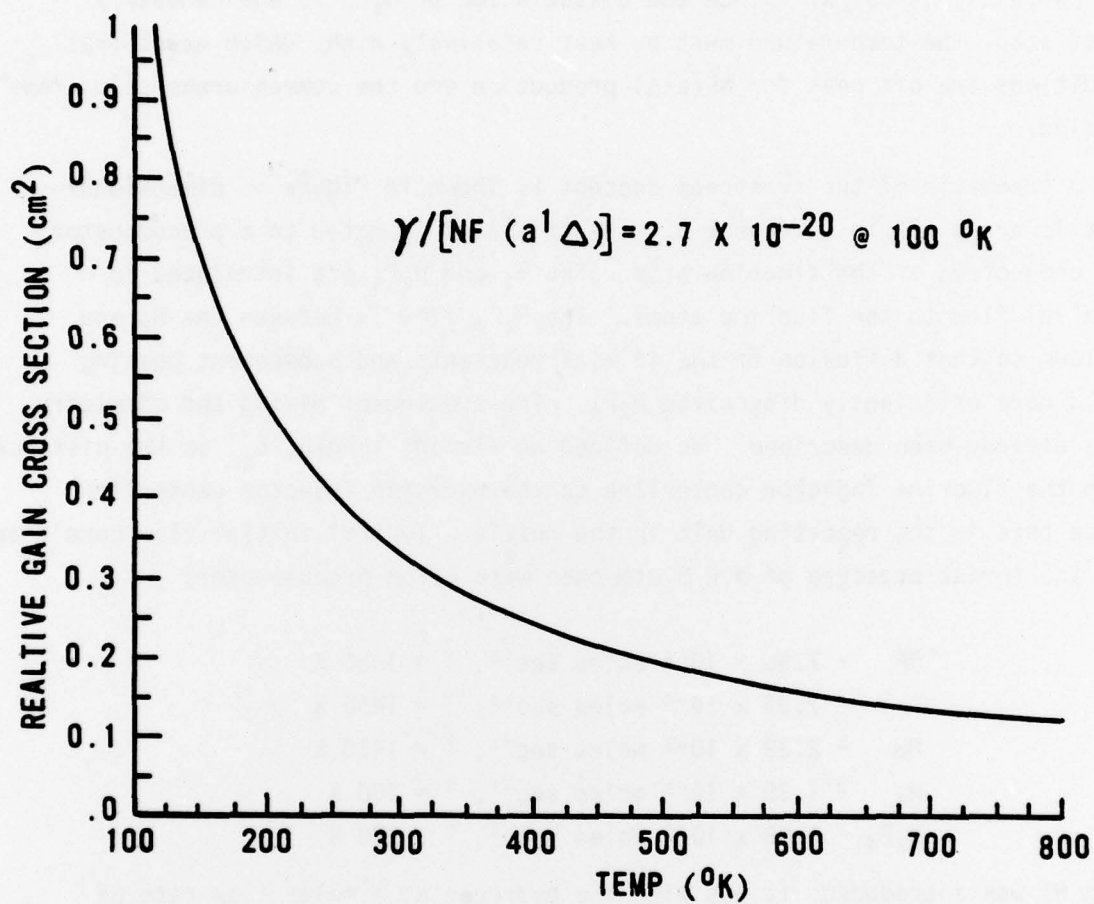


Figure 4. Gain cross section ($\gamma(\text{cm}^{-1})/[NF(a^1\Delta)]$) as a function of temperature.

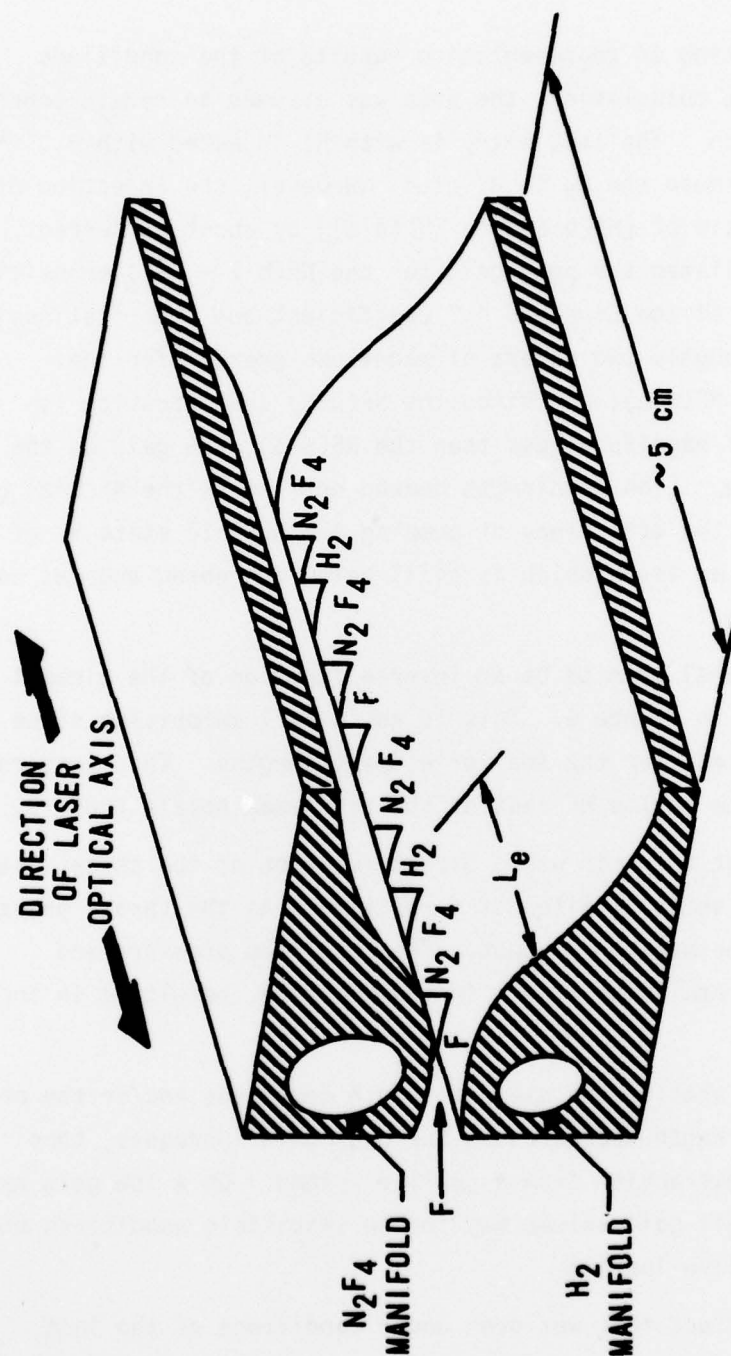


Figure 5. Schematic of the tristream nozzle, showing the reactant gas injection scheme.

SECTION IV

RESULTS AND DISCUSSION

Table 2 is a listing of representative results of the conditions calculated. For this calculation, the area was assumed to remain constant after nozzle expansion. The last entry is with HI injected with H_2 . This lowers the result because the H_2 is diluted. However, the injection of HI does increase the ratio of $[NF(b^1\Sigma)]$ to $[NF(a^1\Delta)]$ by about 50 percent. We have not explicitly listed the peak gain for the $NF(b^1\Sigma \rightarrow X^3\Sigma)$ transition. However, the product of the Einstein "A" coefficient and the rotational dilution factor is roughly two orders of magnitude greater for the $NF(b^1\Sigma)$ than for the $NF(a^1\Delta)$; and since the $NF(b^1\Sigma)$ concentration is roughly two orders of magnitude less than the $NF(a^1\Delta)$, the gain on the two systems is comparable. (The wavelength dependence lowers the $NF(b^1\Sigma)$ gain by ~ 4.0 .) Obviously the efficiency of pumping the $NF(b^1\Sigma)$ state is of critical importance, an issue which is still being addressed and has not yet been resolved.

We found the $NF(a^1\Delta)$ gain to be an inverse function of the element length (L_e) as shown in figure 6. This is not at all surprising since the mixing is more efficient for the smaller element lengths. This same result was seen by Rocketdyne in the HF test of the tristream nozzle (ref. 3).

We also found that the gain was a direct function of the throat pressure (figure 7), a result which is also not surprising. As the throat pressure increases, so does the mass throughput. The resultant pressure and temperature increase manifests itself in the kinetics, resulting in increased gain.

It is also clear that as the element length decreases and/or the pressure increases, the gain length decreases as the peak gain increases, thus necessitating power extraction from a smaller volume. On a low gain system such as this, the small gain volume may impose impossible conditions on the mirrors due to excessive loading.

An interesting effect that was seen under conditions of the last entry in table 2 was a shoulder on the leading edge of the gain curve (figure 8). The effect was small and thought to be an artifact of the

TABLE 2. REPRESENTATIVE RESULTS OF THE MODEL OF NF CHEMISTRY IN THE TRISTREAM NOZZLE

| Expansion Ratio | Throat Pressure (ATM) | Cavity Pressure at Peak Gain Position (Torr) | Temperature (K) at Peak Gain Position | $(NF(a^1\Delta))$ at Peak Gain Position | $(NF(B^1\Sigma))$ at Peak Gain Position | Peak NF ($a^1\Delta-X^3\Sigma$) Gain (cm^{-1}) |
|-----------------|-----------------------|--|---------------------------------------|---|---|--|
| 20 | 10 | 319 | 437 | 6.1×10^{16} | -- | 2.6×10^{-4} |
| 10 | 10 | 448 | 441 | 5.7×10^{16} | -- | 3.6×10^{-4} |
| 10 | 5 | 221 | 446 | 4.2×10^{16} | -- | 3.6×10^{-4} |
| 20 | 10 | 217 | 391 | 4.1×10^{16} | -- | 2.7×10^{-4} |
| 20 | 5 | 108 | 391 | 2.3×10^{16} | -- | 1.6×10^{-4} |
| 10 | 0.5 | 40 | 579 | 4.3×10^{15} | 1.6×10^{13} | 2.5×10^{-5} |
| 10 | 0.5 | 21 | 456 | 2.8×10^{15} | 1.4×10^{13} | $2.0 \times 10^{-5} *$ |
| 10 | 2 | 80 | 640 | 4.9×10^{16} | -- | $1.9 \times 10^{-4} **$ |

Initial conditions: $L_e = 0.095$, $T_F = 1450$ K, $T_{N_2} = 300$ K

* HI Injected with H_2

** H_2 injected at 800 K, laminar mixing assumed.

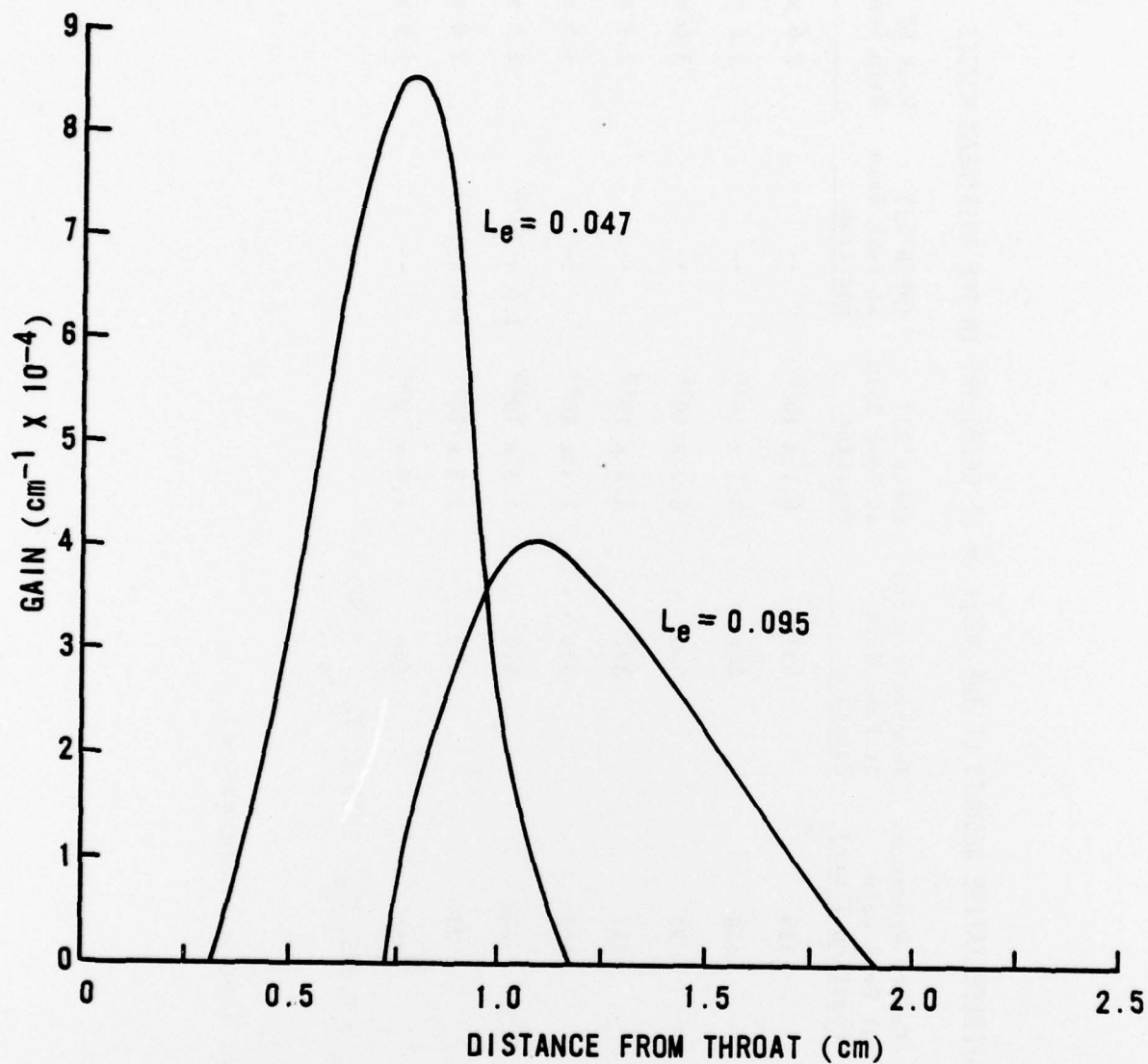


Figure 6. Gain profile as a function of distance from nozzle throat for two element lengths (L_e).

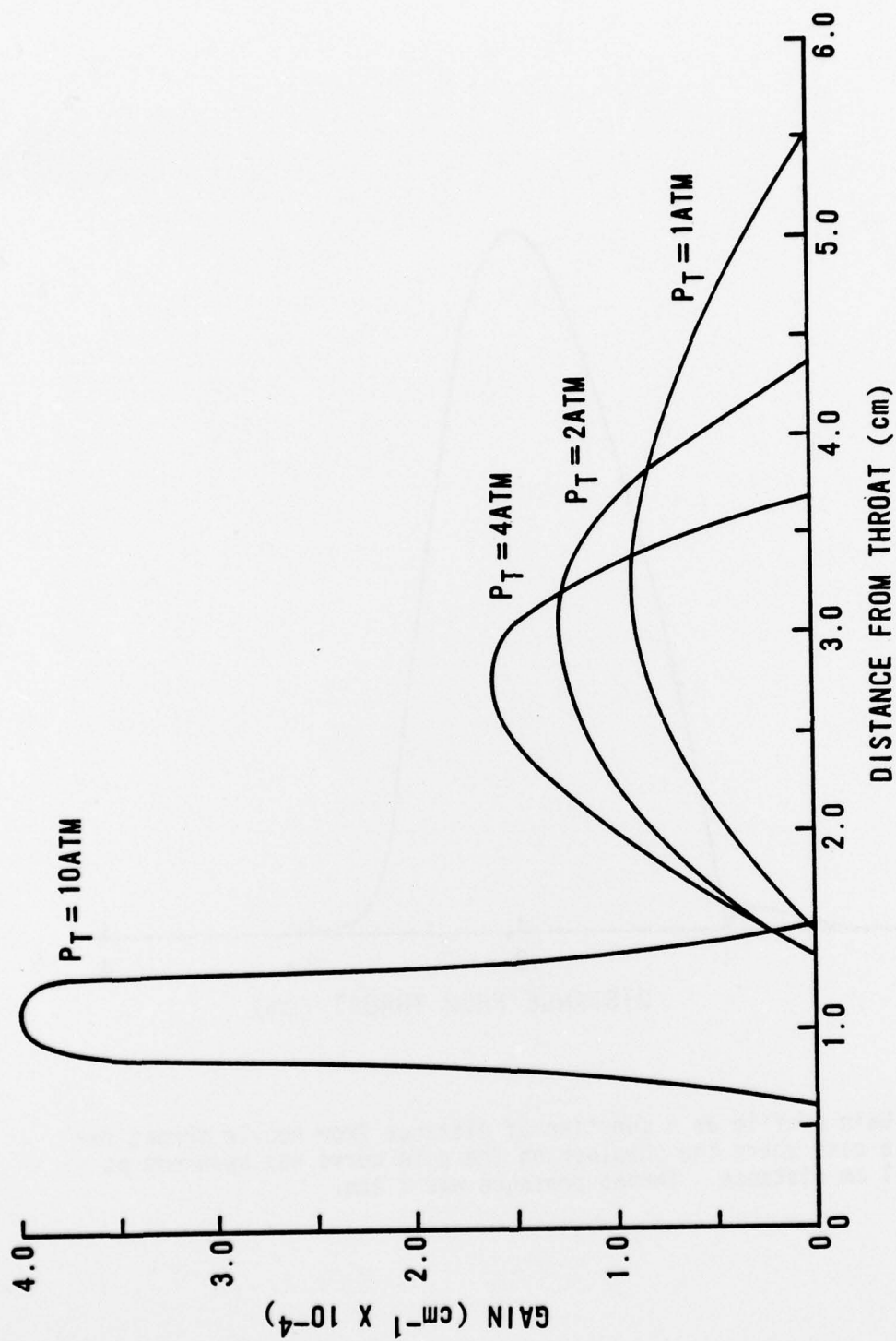


Figure 7. Gain profile as a function of distance from nozzle throat for several throat pressures.

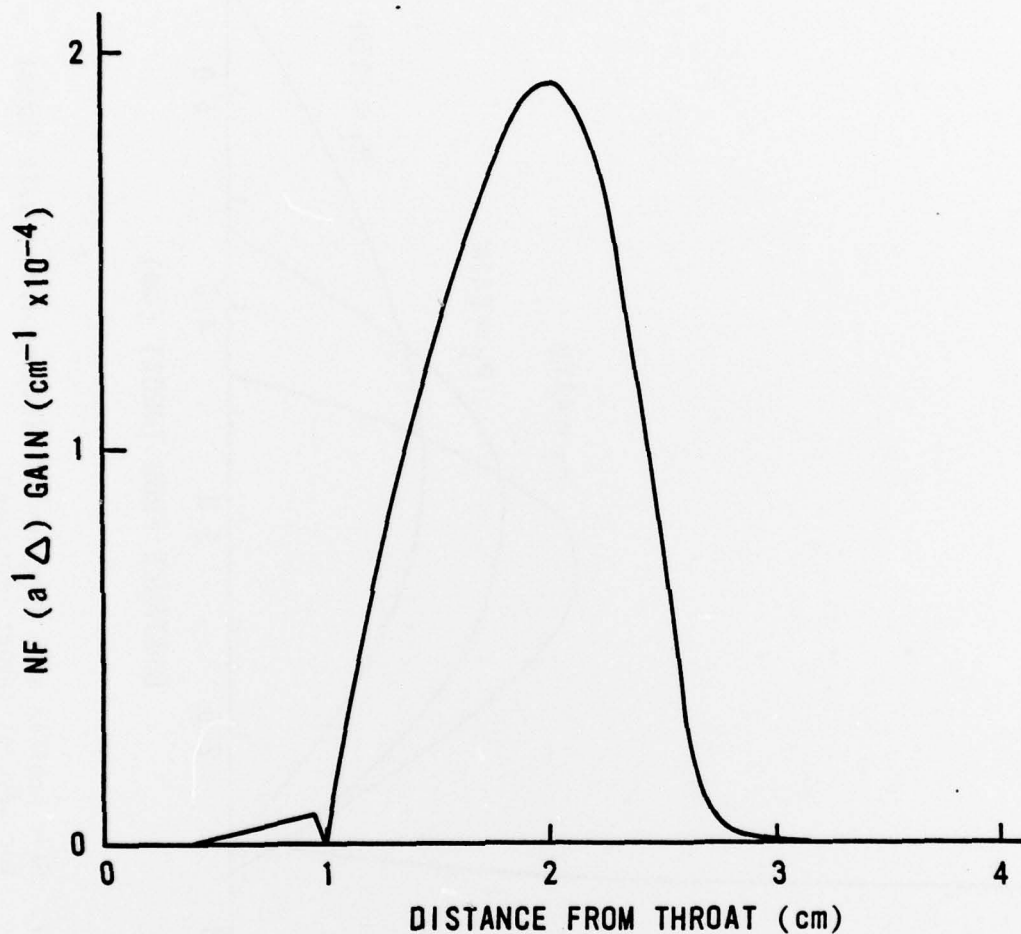


Figure 8. Gain profile as a function of distance from nozzle throat for a case where the shoulder on the gain curve was apparent at 1 cm distance. Throat pressure was 2 atm.

calculation. However, Miller and Betts* have seen the same effect with a different nozzle configuration, indicating that the effect is real. The apparent explanation came out of discussions of the effect between the authors and Betts and Miller. Reaction 22 in table 1 indicates the rate of $N_2F_4 + M$ reaction. If M is another N_2F_4 molecule, then a small amount of the N_2F_4 is predissociated before injection. The ensuing chemistry of the NF_2 occurs more rapidly than the initial N_2F_4 dissociation in the nozzle. Once the initial NF_2 is utilized, the gain drops while the bulk of the N_2F_4 is dissociated, giving rise to the dip in the curve.

Calculations were also performed with the expansion ratio of the nozzle continuing out into the cavity. The reason for doing this is that most of the constant cross section area runs indicated choking as the temperature and pressure built up. The continuance of the expansion ratio alleviated the problem. As expected, the gain length increased and the peak gain decreased.

The main result of the calculation to date is that the tristream concept is very promising; and if the experimental results of TRW verify our model, calculations for scaling will begin. The tristream nozzle as it now exists will not demonstrate lasing because of the short transverse path length (5 cm). However, a longer path tristream nozzle of approximately 50 cm should lase, if our model is correct.

*D. Miller, J. Betts, Presentation of Technical Progress to AFWL, April 1978.

REFERENCES

1. Herbelin, J. M., "The Role of Electron Spin in the NF Kinetic System," Chem. Phys. Lett., 42 (2), 376, 1976.
2. Herbelin, J. M., Kwok, M. A., and Spencer, D. J., "Electronic Transition Lasers," M.I.T. Press, p. 96, Cambridge, MA, 1977.
3. Dickerson, R. A., Zajac, L. J., and Hurlock, S. C., Chemical Laser Advanced Nozzle Development, AFWL-TR-76-45, 1976.
4. Theones, J., et al., Advanced Laser Flow Analysis (ALFA) Theory and User's Guide, AFWL-TR-78-19, 1979
5. Betts, J. A., Advanced Laser Concepts, AFWL-TR-77-234, 1977.
6. Blauer, J. A., Janiak, D., Solomon, W. C., "Electronic Transition Lasers," M.I.T. Press, p. 283, Cambridge, MA, 1977.
7. Cohen, N., Bott, J. F., A Review of Rate Coefficients in the H₂-F₂ Chemical Laser System, SAMSO TR-0076-(6603)-2, 1978.
8. Herbelin, J. M., Chemically Pumped Visible and Infrared Electronic Transition Lasers, ATM 76 (6240-40)-1, 1976.